Journal of Structural Geology 32 (2010) 464–477

Contents lists available at ScienceDirect

Journal of Structural Geology

journal homepage: www.elsevier.com/locate/jsg

# Andean sinistral transpression and kinematic partitioning in South Georgia

Michael L. Curtis [a,*], Michael J. Flowerdew [a], Teal R. Riley [a], Martin J. Whitehouse [b], J. Stephen Daly [c]

[a] British Antarctic Survey, Madingley Road, Cambridge CB3 0ET, UK
[b] Swedish Museum of Natural History, Box 50007, S-104 05 Stockholm, Sweden
[c] UCD School of Geological Sciences, University College Dublin, Belfield, Dublin 4, Ireland

ARTICLE INFO

*Article history:*
Received 16 October 2009
Received in revised form
26 January 2010
Accepted 17 February 2010
Available online 23 February 2010

*Keywords:*
Geochronology
Fold appression
Back-arc basin
Polyphase deformation

ABSTRACT

The island of South Georgia exposes remnants of a Late Jurassic to Early Cretaceous Andean magmatic arc and marginal basin system that was compressively deformed during the mid-Cretaceous main Andean Orogeny forming widespread NW-SE trending folds and a coaxial penetrative cleavage displaying a predominantly NE-SW stretching lineation.

Detailed structural studies of the Cooper Bay to Cape Vahsel area of South Georgia reveal that intense, mid-Cretaceous, polyphase deformation was strongly influenced by sinistral strike-slip shear parallel to the NW-SE regional structural grain, and along a major pre-existing fault, which we interpret as the partitioned wrench component of bulk transpressional deformation. The relationship between fold axial plane orientation and interlimb angle of widely distributed mesoscale folds is consistent with counter-clockwise rotation and fold appression as a result of sinistral simple shear deformation, suggesting kinematic strain partitioning of the wrench component was on the whole highly efficient. Locally, the modification of steep tectonic anisotropies to shallow inclinations during $D_2$ deformation induced imperfect or inefficient partitioning with fold arrays exhibiting fold appression characteristic of a transpressional deformation path.

Our partitioned transpression model for main Andean deformation of South Georgia fits well with tectonic interpretations of the Cordillera Darwin, Patagonia.



## 1. Introduction

The island of South Georgia lies approximately 1800 km east of the southern tip of South America along the Scotia arc, which forms a complex locally emergent submarine ridge linking the southernmost Andes, via South Georgia, the South Sandwich Islands volcanic arc, South Orkney and South Shetland Islands, and finally the Antarctic Peninsula (Fig. 1). Established stratigraphical, igneous and tectonic correlations between South Georgia and Tierra del Fuego (e.g. Dalziel et al., 1975; Tanner, 1982; Thomson et al., 1982; Macdonald et al., 1987; Mukasa and Dalziel, 1996) together with tectonic reconstructions (e.g. Livermore et al., 2007) indicate that, prior to the Late Oligocene to recent evolution of the Scotia Sea, South Georgia was situated at the southern tip of South America where it formed an extension of the Andean magmatic arc and marginal basin system (Dalziel et al., 1975; Tanner, 1982; Mukasa and Dalziel, 1996).

The elongate, Late Jurassic to Early Cretaceous Andean marginal basin exposed in southernmost Patagonia and South Georgia is known as the Rocas Verdes marginal basin (Dalziel, 1981; Dott et al., 1982; Olivero and Martinioni, 2001; Fildani and Hessler, 2005), and has been linked with the initial opening of the Weddell Sea (Dalziel, 1992; König and Jokat, 2006). During the late-Early Cretaceous to mid-Cretaceous a combination of increased sea-floor spreading rates and a change in the South American pole of rotation relative to Africa is considered to have increased the convergence rate between the Pacific and South American plates (Dalziel, 1986), resulting in the compressive deformation and inversion of the Rocas Verdes basin during the mid-Cretaceous main Andean Orogeny (Dalziel, 1981; Nelson, 1982; Suárez et al., 2000). In South Georgia mid-Cretaceous deformation is manifest as widespread and locally intense folding of the Early Cretaceous basin fill deposits, and their juxtaposition against basement rocks of the Drygalski Fjord Complex along a regional shear zone referred to as the Cooper Bay Dislocation Zone (Tanner, 1982).

In this contribution we present new structural, kinematic and geochronological data from the Cooper Bay–Cape Vahsel region of South Georgia, providing a detailed model for the kinematic evolution of the adjacent basin fill deposits which are strongly influenced by a component of sinistral wrench tectonics. We propose that the main Andean deformation of South Georgia was

* Corresponding author. Tel.: +44 (0)1223 221429.
*E-mail address:* m.curtis@bas.ac.uk (M.L. Curtis).

0191-8141/$ – see front matter 
doi:10.1016/j.jsg.2010.02.002

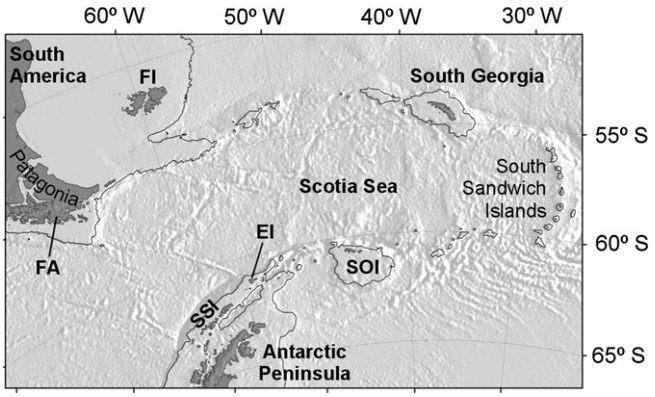


**Fig. 1.** Map of the present day Scotia Arc. FI – Falkland Islands, FA – Fuegian Andes, SSI – South Shetland Islands, SOI – South Orkney Islands, EI – Elephant Island. Shaded bathymetric relief reveals gross structure of Scotia Sea floor. Continuous black line is the 1000 m bathymetric contour.

transpressional in character, with efficient kinematic strain partitioning focussing the wrench component along a pre-existing major tectonic boundary. Our results emphasise the potential influence of pre-existing zones on weakness and evolving tectonic fabrics on kinematic strain partitioning, as well as strengthening tectonic correlations between South Georgia and the Fuegian Andes of southernmost South America.

## 2. Geology and stratigraphy of South Georgia

The southern tip of South Georgia is composed of two basement complexes, separated by an inferred fault (Fig. 2) (Macdonald et al., 1987). The Drygalski Fjord Complex (DFC) is characterised by an assemblage of highly deformed paragneisses and metasedimentary rocks that are intruded by extensive tholeiitic plutons (Storey, 1983). Age constraints within the DFC are poor, with K-Ar dates from olivine gabbros suggesting an Early Jurassic age (Tanner and Rex, 1979). The Larsen Harbour Complex (s.s. Macdonald et al., 1987) is interpreted to be an ophiolite sequence representing the local development of mafic oceanic crust (Storey et al., 1977; Mair, 1987) prior to 150 ± 1 Ma (Mukasa and Dalziel, 1996). Together, this basement assemblage is interpreted as a Gondwana margin accretionary complex, of uncertain age, that underwent crustal thinning during Middle to Late Jurassic times (Storey, 1983; Macdonald et al., 1987; Mukasa and Dalziel, 1996), and is inferred to underlie much of the island.

The remainder and majority of the rock exposure on South Georgia is formed by two laterally equivalent turbidite sequences deposited in an Early Cretaceous back-arc basin. The Cumberland Bay Formation contains diagnostic Early Cretaceous marine macrofossils (Thomson et al., 1982) and forms an 8 km thick succession of andesitic volcaniclastic greywackes derived from a volcanic island arc, while the more siliciclastic Sandebugten Formation is inferred to be contemporaneous and derived from the continental margin of the back-arc basin (Dalziel et al., 1975; Stone, 1980; Tanner, 1982). A third metasedimentary succession, the Cooper Bay Formation, is restricted to the most southeasterly promontory of South Georgia and based on geochemical data is considered to be a facies variant of the Cumberland Bay Formation, albeit derived from a more basic source (Clayton, 1982).

Deformation of the greywacke sequences occurred predominantly at low metamorphic grade, prehnite–pumpellyite facies along the northeast coast of the island (Skidmore, 1972; Stone, 1980) increasing to biotite zone of greenschist facies in the Cooper Bay Formation adjacent to the Drygalski Fjord Complex (Stone, 1982; Storey, 1983; Macdonald et al., 1987). Large scale,

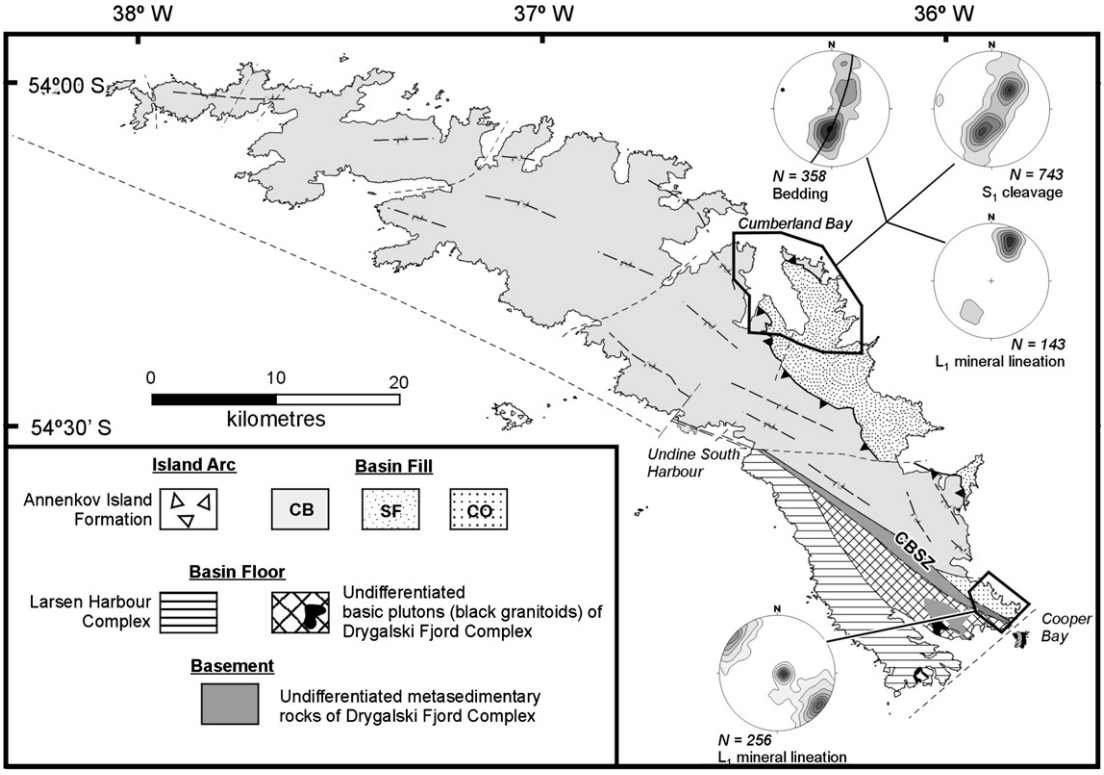


**Fig. 2.** Simplified geological map of South Georgia highlighting the main stratigraphical divisions, tectonic components and structural trends. Based on Macdonald et al. (1987). CB – Cumberland Bay Formation, SF – Sandebugten Formation, CO – Cooper Bay Formation, CBSZ – Cooper Bay Shear Zone. Stereograms of planar and linear $D_1$ structural data from the Cumberland Bay and Cooper Bay areas revealing contrasting regional kinematics.

northwest–southeast trending chevron folds dominate the Early Cretaceous greywacke successions with a predominantly north-northeast–south-southwest mineral lineation developed along a ubiquitous axial planar cleavage (Tanner, 1982; Tanner and Macdonald, 1982). K-Ar whole rock dating of geographically widespread slate samples from the Cumberland Bay and Sandebugten formations range between 51 and 135 Ma, with a best estimate for the minimum age of deformation and metamorphism being 82–91 Ma (Thomson et al., 1982). This estimate is consistent with the geological history of the Rocas Verdes marginal basin of southern Patagonia, the contiguous region to South Georgia in palinspastic reconstructions, suggesting that the Early Cretaceous back-arc basin fill of South Georgia was deformed during the mid-Cretaceous main Andean orogeny (e.g. Dalziel et al., 1975; Bruhn and Dalziel, 1977; Nelson et al., 1980; Nelson, 1982; Cunningham, 1995; Suárez et al., 2000).

One of the most significant structural components of the South Georgia microcontinental block is the regional scale Cooper Bay Shear Zone, previously referred to as the Cooper Bay Dislocation Zone (Macdonald et al., 1987), which juxtaposes the Early Cretaceous greywacke successions against the basement complexes. Previous geological studies have revealed this 'dislocation zone' has a complex tectonic history displaying both dip-slip and strike-slip mineral lineations that was linked to the structural evolution of the adjacent Cooper Bay Formation (Stone, 1982; Storey, 1983). The structural and kinematic evolution of the Cooper Bay Formation and adjacent shear zones forms the basis of this study.

## 3. Structural evolution of the Cooper Bay to Cape Vahsel areas

The Cooper Bay Formation crops out in the south-eastern promontory of South Georgia, between the Quensel, Leward and Twitcher glaciers and Cape Vahsel (Fig. 3). Previous workers revealed the Cooper Bay Formation to be characterised by regional metamorphism up to the biotite grade of greenschist facies with a polyphase deformation history linked, to some extent, to the development of mylonitic fabrics within the adjacent Cooper Bay Dislocation Zone (Stone, 1982; Storey, 1983) or, as we propose it should be more appropriately referred to, the Cooper Bay Shear Zone (CBSZ).

Geological mapping conducted for this study also identified a previously unrecognised shear zone trending sub-parallel to the CBSZ that is wholly developed within the Cooper Bay Formation, and will be referred to as the Cape Vahsel Shear Zone. Due to the intimate relationship between the deformed Cooper Bay Formation and bounding shear zones, we first present structural and kinematic field data from the shear zones.

### 3.1. Cooper Bay Shear Zone

The Cooper Bay Shear Zone (CBSZ) encompasses an elongate belt of generally highly strained igneous and metasedimentary rocks, trending N126°E, extending for almost 50 km from Cooper Bay to Undine South Harbour (Macdonald et al., 1987). The CBSZ juxtaposes basic plutons and metasedimentary rocks of the Drygalski Fjord Complex along its southwest flank against highly deformed metagreywacke and metabasic rocks of the Cooper Bay Formation along its northeast flank (Storey, 1983). Stone (1982) and Storey (1983) revealed the "dislocation zone" has a complex tectonic history displaying both dip-slip and strike-slip mineral lineations, with a major component of inferred vertical, north-easterly directed reverse displacement, proposed to account for the stratigraphical juxtaposition (Storey, 1983; Macdonald et al., 1987).

The field data reported here are based on the re-examination of several localities along a 6 km trace of CBSZ's length, as well as extensive mapping around Cooper Bay. It considerably expands the limited data presented by Curtis (2007) which confirmed the structural and kinematic differences present within the opposing margins of the CBSZ and also identified a sinistral strike-slip component.

#### 3.1.1. Northeast margin

From its inferred tectonic contact with the Drygalski Fjord Complex, the Cooper Bay Formation exhibits a 250–700 m wide zone of ductile shearing that is characterised by pale-green, white

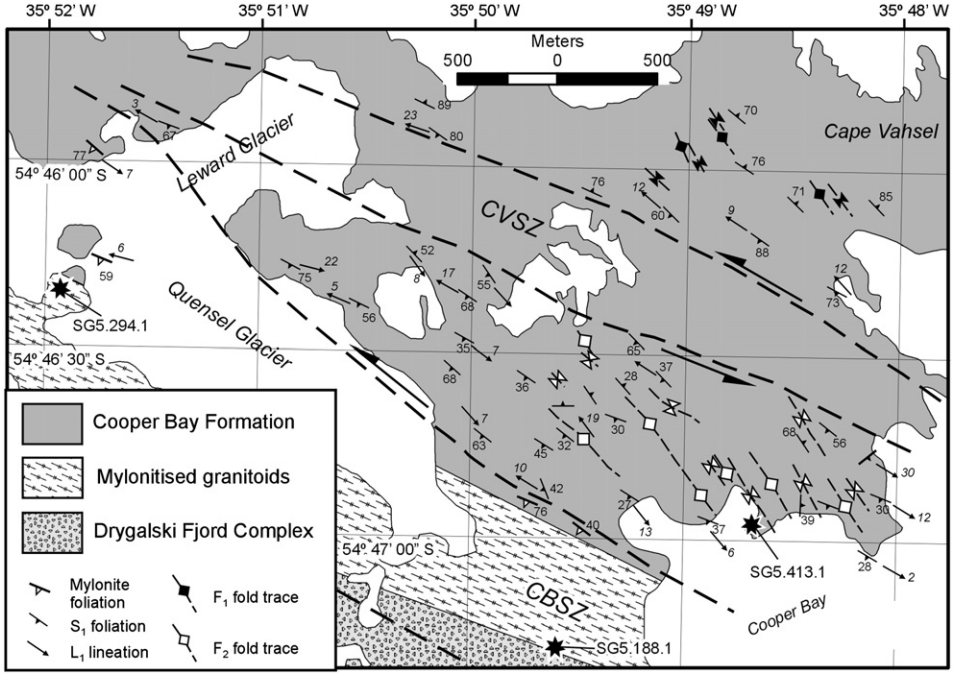


**Fig. 3.** Simplified structural geology map of the Cooper Bay – Cape Vahsel – Quensel Glacier area displaying the main structural features of the Cooper Bay Formation. Heavy dashed lines are the margins of regional shear zones: CBSZ – Cooper Bay shear zone, CVSZ – Cape Vahsel Shear Zone.

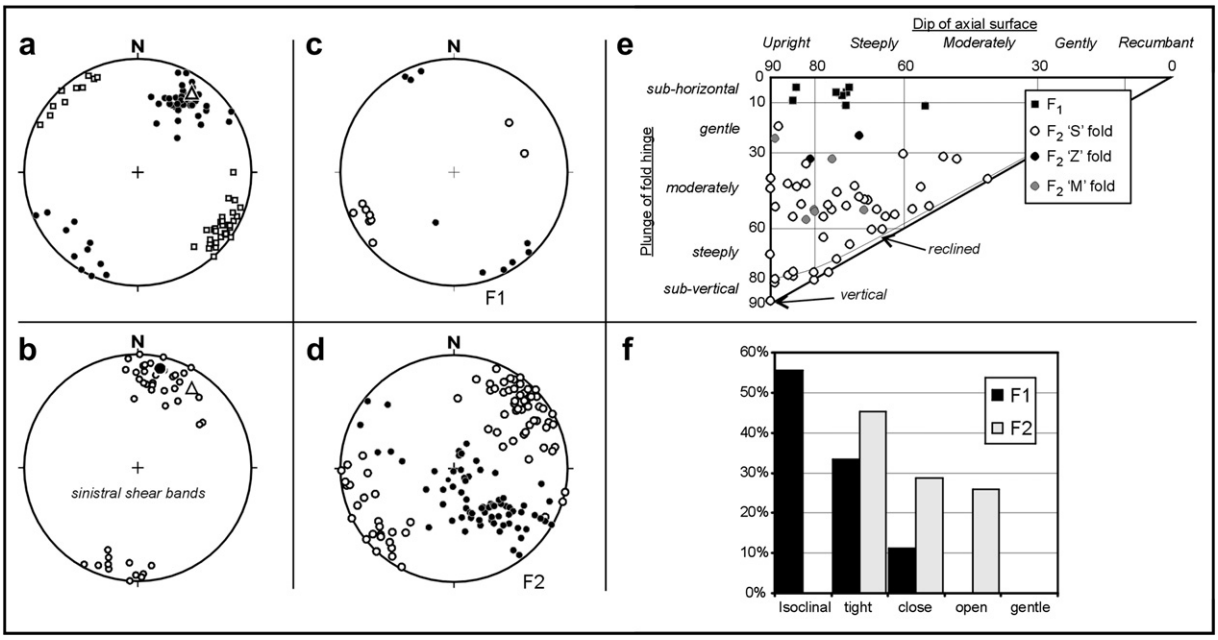


**Fig. 4.** Structural data from northeast margin of Cooper Bay Shear Zone. a) Black circles – poles to mylonite foliation, open squares – lineation on mylonite foliation. Open triangle – mean mylonite foliation. b) Poles to C′-type sinistral shear bands. Open triangle – mean pole to mylonite foliation, black circle – mean C′-type shear band. c) Open circle – pole to F1 fold axial plane, closed circle – F1 fold axis. d) Open circle – pole to F2 fold axial plane, closed circle – F2 fold axis. e) Plot of fold axial surface dip against plunge of fold hinge highlighting range of fold attitudes. f) Percentage frequency distribution of fold interlimb angles for F1 and F2 fold.

and black banded mylonite that gives way toward the northeast to less highly deformed metasedimentary and metabasic schist and phyllite. The margin of the shear zone was established where typical compositional banding within the metasedimentary rocks of the Cooper Bay Formation was identifiable.

The mylonitic foliation has a mean orientation of 214/72, displaying a pronounced strike-parallel quartz mineral lineation with a mean orientation of 127/06° (Fig. 4). Numerous sinistral C′-type shear bands (Berthé et al., 1979; White et al., 1980) form a mean 22° counter-clockwise relationship with the mylonite fabric demonstrating a sinistral sense of shear along the CBSZ (Curtis, 2007).

The mylonite fabric displays evidence for two generations of folds. Rare, early generation folds are predominantly tight to isoclinal, with upright to steeply inclined axial planes oriented subparallel to the mean mylonite foliation, with sub-horizontal fold hinges (Fig. 4c and e). The later generation of folds range in interlimb angle from open to tight, and are predominantly upright to steeply inclined (Fig. 4d and e). These younger folds exhibit a systematic counter-clockwise rotation of their fold axial plane relative to the shear zone strike with increasing fold tightness, a relationship indicative of a sinistral non-coaxial strain that is discussed in greater depth in Section 5.1 (see Fig. 13).

Fold hinge orientation within the later fold generation displays a wide, asymmetric distribution from gently plunging to sub-vertical, via southeasterly, moderate plunging folds (Fig. 4d). Fold symmetry is dominated by 'S'-folds, particularly the steep- to vertically-plunging fold population, which exhibits almost exclusively sinistral verging 'S' folds (Fig. 4e). We interpret the asymmetric distribution of fold hinges and fold symmetry to indicate a general curvilinear hinge geometry within the fold population, although the median closing direction is not parallel to the mylonite lineation (Fig. 5).

### 3.1.2. Southwest margin

The southwestern margin of the CBSZ affects the diverse lithologies of the Drygalski Fjord Complex. At Cooper Bay, extensive coastal exposures of gabbro and diorite are heterogeneously sheared into zones of augen-, proto- and meso-mylonite, up to 130 m wide. The mylonite foliation has a mean orientation of 214/73 but does not generally display a mineral lineation, although where locally developed it is predominantly down-dip (Fig. 6) (Curtis, 2007).

The mountain ridges forming the southwestern flank of the Quensel and Leward glaciers expose multiple sheets of porphyritic granodiorite that intrude the Drygalski Fjord Complex. The granodiorite sheets are generally medium to coarse grained and vary in thickness from a metre to several metres. Protomylonite textures dominate the granite sheets, with even the least strained granites displaying lozenge shaped quartz and kinked biotite phenocrysts. Occasionally northeastly directed reverse shear indicators were observed in outcrop. In addition to the broad low-strain zones, rare, narrow (<1 m) zones of meso- to ultramylonite were also encountered, exhibiting a down-dip mineral lineation and abundant microstructural evidence (e.g. extensional shears bands and σ-prophyoroclasts) indicating a top-down to the southwest, normal sense of shear (Fig. 7).

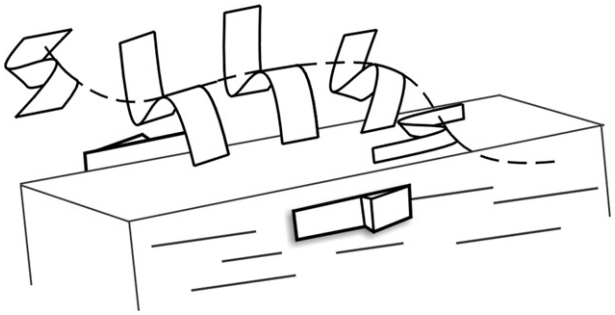

**Fig. 5.** Range of most common mesoscale fold attitudes and symmetry within the mylonites of the northeast margin of the CBSZ, relative to main elements of the mylonite fabric. Folds may represent a general curvilinear fold hinge geometry. Very similar fold geometries are encountered throughout the study area.

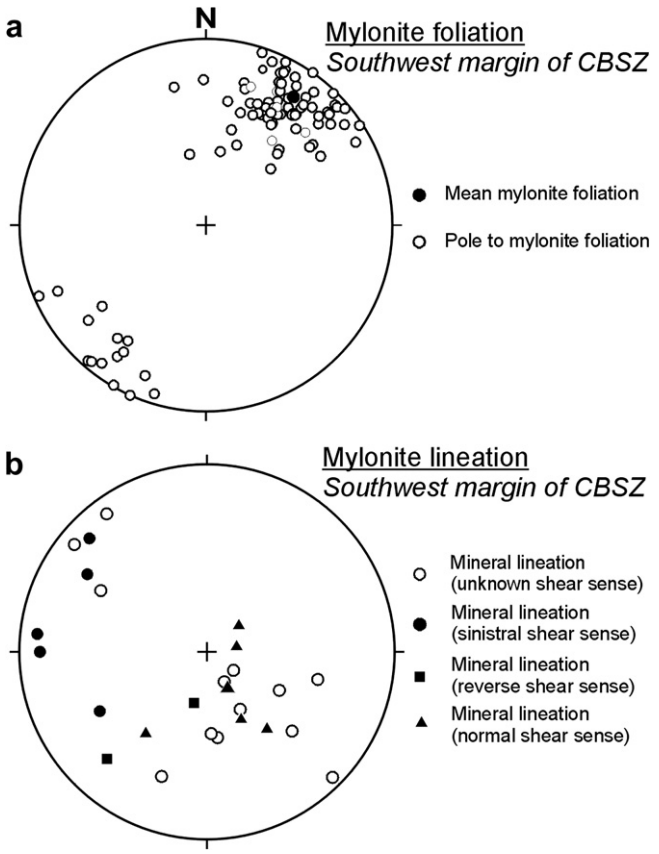


**Fig. 6.** Stereograms of a) poles to mylonite foliation, and b) lineations along mylonite surface differentiated according to shear sense, if known. Southwest margin of the CBSZ within rocks of the Drygalski Fjord Complex.

Evidence for localised sinistral strike-slip shear was encountered at several localities along the southwest margin of the CBSZ, where thin bands of metabasic schists and chloritic pelites/semi-pelites display well-developed sinistral C′-type shear bands. In addition to these zones of rheological contrast or weakness, several thin (<20 cm wide) sinistral mylonite zones were encountered cutting porphyritic granodiorite exposed at the northeast end of the Leward Glacier.

### 3.1.3. Faulting

Curtis (2007) reported the presence of at least 31 faults within the studied area of the CBSZ, 83% of which are approximately NW–SE striking, sub-parallel to the main shear zone (Fig. 8). The faults are characterised by narrow damage zones composed of fault breccia and protocataclasite. Shear sense was determined on 16 faults, all of which displayed identifiable left-lateral offsets varying between 3 cm and 12 m. A subordinate set of ENE–WSW trending, strike-slip faults is also present, two of which also display a sinistral sense of displacement.

The brittle fault population is widely distributed across the extent of the CBSZ, in areas displaying sinistral ductile shear, as well as the southwestern margin where down-dip ductile shear kinematics predominate. The presence of sinistral cataclastic faults, at the expense of down-dip faults, suggests that left-lateral displacement along the CBSZ spanned its exhumation through the brittle/ductile transition.

## 3.2. Cape Vahsel Shear Zone

Systematic mapping of the Cooper Bay Formation revealed the presence of a previously unidentified N114°E trending shear zone, extending for at least 4.2 km northwest from the coast between Cooper Bay and Cape Vahsel to the Leward Glacier, which is up to 560 m wide (Fig. 3). This newly identified shear zone, the Cape Vahsel Shear Zone (CVSZ), is characterised by a sub-vertically dipping phyllitic foliation, that is sheared into a sigmoidal 'Z'-shaped geometry by the widespread development of sinistral C′-type shear bands, the length and spacing of which vary up to 30 cm. A strike-parallel lineation is occasionally present on both the phyllitic foliation plane and the shear bands (Fig. 9).

In addition to the shear bands, rare centimetre-scale NW–SE trending folds are present. Although the dataset is small, the range of fold attitudes are similar to those in the CBSZ, ranging from tight, sub-horizontal upright folds, via southeasterly moderate plunges to close, steeply-plunging, upright folds, that display a predominantly 'S'-shaped symmetry (Fig. 9). Fold axial planes form a mean

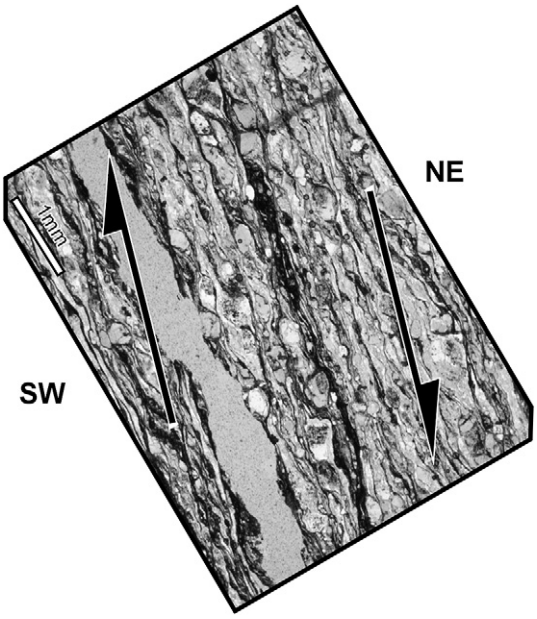


**Fig. 7.** C/S mesomylonitic fabric developed within narrow shear zone indicating an apparent extensional sense of shear.

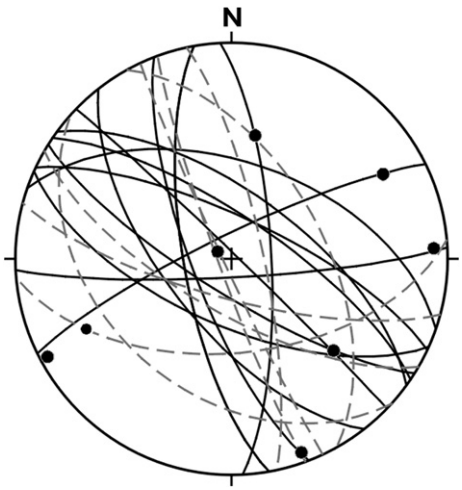


**Fig. 8.** Stereogram displaying fault planes, plotted as great circles, from the CBSZ. Solid lines – sinistral faults, dashed lines – unknown sense of displacement. Closed circles – slickenlines on fault surface.

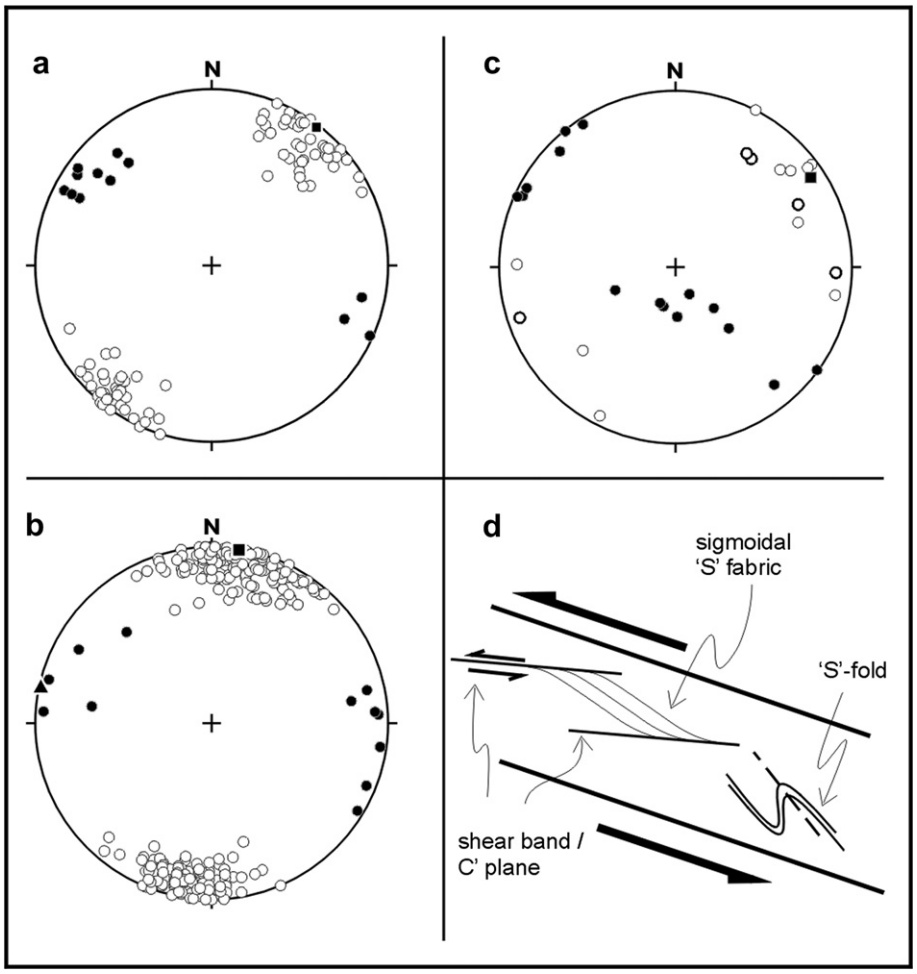


**Fig. 9.** Structural data from the Cape Vahsel Shear Zone. a) Phyllite foliation (poles) – open circles, lineation on phyllite surface – filled circles. Filled square – mean foliation. b) C′-type shear bands (poles) – open circles, lineation along shear band – filled circle. Filled square and triangle – mean shear band and lineation, respectively. c) Fold axial plane (pole) – open circle, fold hinge – filled circle. Mean fold axial plane – filled square. d) Summary of mean orientations of the main structural elements within a sinistral kinematic model for the CVSZ.

clockwise-oblique angle to the shear zone boundary, with the individual angle decreasing with increased fold tightness.

All structural components within the CVSZ display a marked geometric asymmetry relative to the map scale trend of the shear zone. The mean strike of the phyllitic foliation (measured at the centre of its sigmoidal trace) forms a 14° clockwise angle to the shear zone trend, while the sinistral shear bands form a mean 14° counter-clockwise angle (Fig. 9d) typical of C′-type shear bands. The geometric relationship of the phyllite foliation, its 'z'-shaped sigmoidal geometry, abundant C′-type shear bands and clockwise obliquity of minor folds (mean 29°) indicate a strong component of sinistral shear along the CVSZ.

### 3.3. Structure of the Cooper Bay Formation

The Cooper Bay Formation crops out to the northeast of the Cooper Bay shear zone, and is bisected by the newly recognised Cape Vahsel Shear Zone. Its structural style differs markedly either side of the CVSZ, and will be described separately.

#### 3.3.1. Structure of the Cooper Bay Formation to the SW of the Cape Vahsel Shear Zone

The earliest deformation phase identified within the Cooper Bay Formation is the most intense, being characterised by sub-horizontal to gently plunging, tight to isoclinal $F_1$ folds (Fig. 10a–d). Original depositional layering ($S_0$) has been transposed into parallelism with the axial planar cleavage to form a composite foliation ($S_1$), with $S_0$ and $S_1$ only distinguishable within $F_1$ fold hinges. The composite $S_1$ foliation forms shallow to moderately inclined slaty, phyllitic and rarely schistose fabrics that are predominantly defined by chlorite and locally biotite. A pronounced quartz mineral lineation ($L_1$) is developed along thin, $S_1$-parallel, quartz layers, the mean orientation of which (05/129) is sub-parallel to the mean $F_1$ fold axis (07/139) (Fig. 10a).

$D_1$ structures have been refolded about NW–SE trending, macroscale, $F_2$ fold hinges (wavelength c. 300 m) forming a left-stepping, en echelon fold array that is confined between the Cooper Bay and Cape Vahsel shear zones (Fig. 3). Plotted on a stereogram, poles to $S_1$ foliation form a well-defined girdle distribution, the pole to the best-fit great circle ($\pi$-pole) for which indicates the macroscale $F_2$ folds have a mean fold axis plunging 09/138 (Fig. 10a), forming a 12° clockwise-oblique angle to the CBSZ.

In addition to map scale folds, mesoscale (metre scale wavelength) $F_2$ folds are common throughout the area. Although fold attitude is generally upright to steeply inclined, fold hinges display a wide asymmetric distribution of fold plunge from sub-horizontal, through moderate southeasterly plunges, to sub-vertical (Fig. 10b). A small minority of gentle to sub-horizontally plunging, moderate

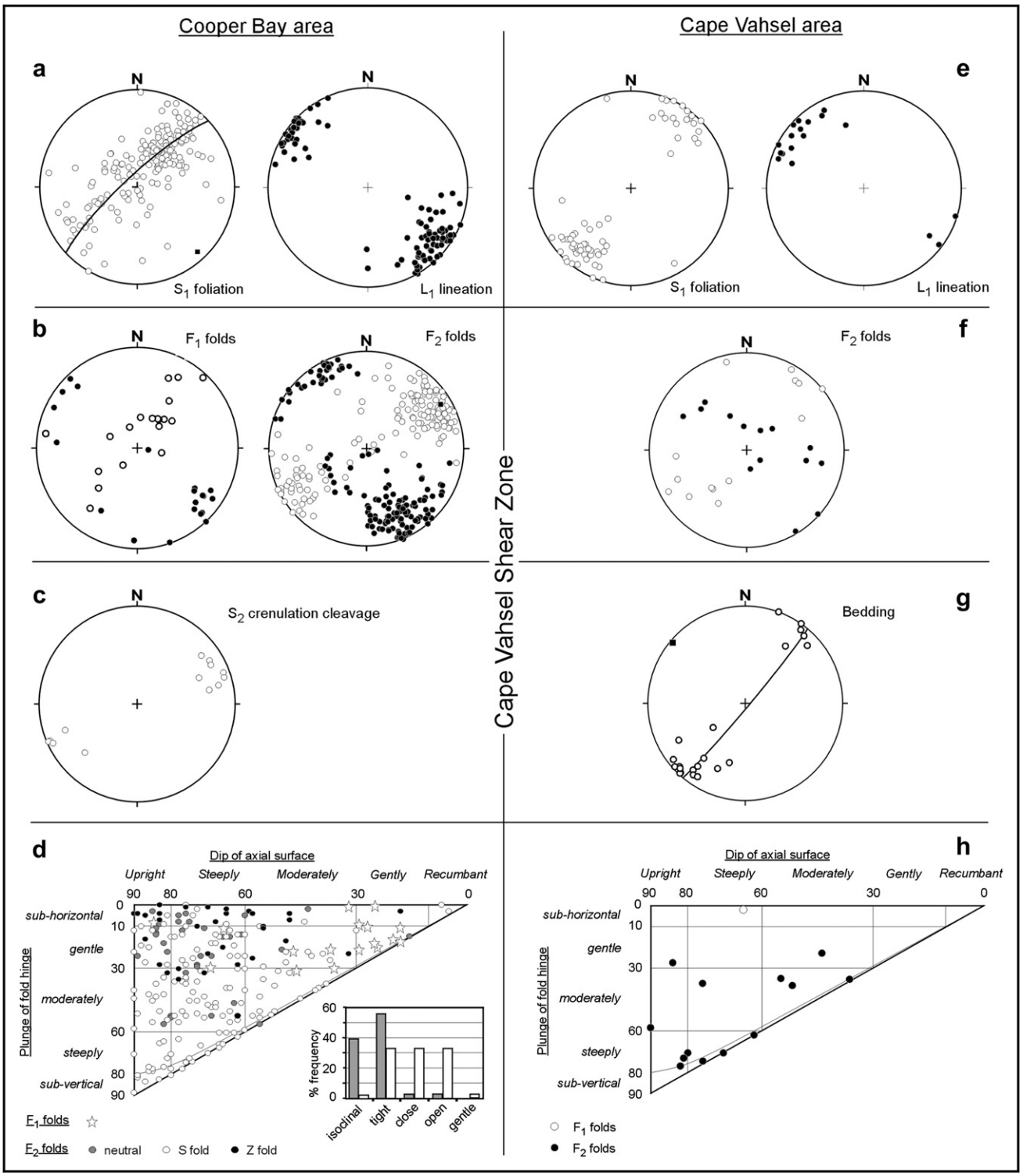


**Fig. 10.** Structural data from the Cooper Bay Formation. Data from the Cooper Bay area, SW of the CVSZ. a) Stereograms displaying poles to $S_1$ foliation (filled square – π-pole, pole to best-fit great circle), and $L_1$ lineations. b) Stereograms displaying poles to F1 and F2 fold axial planes (open circles), and fold hinges (filled circles). c) Poles to S2 crenulation cleavage. d) Plots of 'fold hinge plunge' against 'dip of axial plane' showing the range of fold attitudes in F1 and F2 fold populations (F2 folds are differentiated according to fold symmetry), and percentage frequency distribution of F1 and F2 fold tightness. Data from the Cape Vahsel area, NE of the CVSZ. e) Stereograms displaying poles to S1 foliation (filled square – pole to best-fit great circle), and L1 lineations. f) Stereogram displaying poles to F2 fold axial planes (open circles), and fold hinges (filled circles). g) Poles to sedimentary bedding, with pole to best-fit great circle (filled square). h) Plot of 'fold hinge plunge' against 'dip of axial plane' showing the range of F2 fold attitudes.

to recumbently inclined folds were also encountered. The mesoscale $F_2$ fold population possesses a mean axial plane of 236/81 (22° clockwise-oblique to CBSZ), and mean fold hinge plunging 18/151. In contrast to the tight to isoclinal $F_1$ fold population, mesoscale $F_2$ fold interlimb angles vary between open and tight, with only 18% displaying an axial planar $S_2$ crenulation cleavage (Fig. 10c), the presence of which appears to be restricted to pelitic horizons within the hinge zones of tight to close folds.

If the mesoscale $F_2$ fold population is differentiated according to fold symmetry, systematic differences are revealed (Fig. 10d). Gentle to sub-horizontal plunging folds display a range of fold symmetry (60% S-fold, 22% Z-fold, and 18% neutral folds), whereas folds plunging at >45° are almost exclusively sinistral verging (91% S-shaped, 9% neutral fold).

The broad range of fold symmetries within the gentle to sub-horizontally plunging mesoscale folds are structurally consistent with them being parasitic to the macroscale $F_2$ folds in the Cooper Bay area. However, the fold symmetry of the moderate to sub-vertically plunging folds is generally independent of their position relative to the macroscale $F_2$ folds indicating they are not simple parasitic folds, and may be related to heterogeneous sinistral shear sub-parallel to the bounding regional shear zones.

#### 3.3.2. Structure of the Cooper Bay Formation to NE of the Cape Vahsel Shear Zone

Strain is significantly lower to the northeast of the CVSZ, with both original sedimentary bedding and tectonic cleavage discernible at most localities. The structural style of this area is characterised by macroscale, NW–SE trending, tight, upright to steeply-inclined $F_1$ folds that have a calculated mean fold axis plunging 02/128 (Figs. 3 and 10g). The southwestern limbs of $F_1$ anticlines are generally overturned and a pronounced axial planar cleavage is present throughout the area (Fig. 10e). The $F_1$ folds form a low angle (14°), clockwise-oblique relationship to the CVSZ.

Strain increases with proximity to the northeast boundary of the CVSZ, as evidenced by the obliteration of original sedimentary layering and development of a sub-horizontal stretching lineation within 220 m of the shear zone margin (Figs. 3 and 10e). This increase in strain accompanies an 8° counter-clockwise rotation of the $S_1$ cleavage and, by inference, $F_1$ fold axial surfaces toward the shear zone.

Rare, predominantly tight, decimetre to metre scale, $F_2$ folds are present within the Cape Vahsel area displaying a broad range of fold attitudes, from moderately-plunging and moderately-inclined folds, to steeply-plunging and steeply-inclined (Fig. 10f and h). $F_2$ fold symmetry is almost exclusively 'S'-shaped.

## 4. Geochronology

One biotite bearing schist sample (SG5.413.1) from the Cooper Bay area and two granite samples (SG5.188.1 and SG5.294.1) from within the Cooper Bay shear zone were selected for geochronology in order to constrain the timing of deformation (Fig. 3). The schist has a mineral assemblage of biotite–quartz–plagioclase–titanite–opaques. Biotite forms an $S_1$ foliation which has been crenulated during $D_2$. There is little or no mineral growth after $D_1$. Rb-Sr biotite geochronology places a minimum age constraint on the deformation, while the U-Pb geochronology places both a maximum age constraint of the deformation as well as constraining the magmatic evolution within the Drygalski Fjord Complex.

### 4.1. Rb-Sr biotite geochronology

Rb-Sr analyses for biotite and titanite from sample SG5.413.1 (Table 1) were undertaken at the School of Geological Sciences, University College Dublin, Ireland. 99% Pure handpicked mineral separates (c. 0.03 g) were spiked with a mixed $^{85}Rb$-$^{84}Sr$ spike and dissolved in a 5:1 HF and $HNO_3$ acid mixture. Chemical separation of Sr used TruSPEC resin whilst separation of Rb used traditional chromatography. Rb and Sr were analysed on modified VG Micromass 30 and VG 354 thermal ionisation mass spectrometers, respectively. Rb/Sr uncertainty is estimated to be 1.5% based on repeat analysis of the SRM 607K-feldspar standard, while the

**Table 1**
Rb-Sr mineral data.

| Mineral | Rb (ppm) | Sr (ppm) | $^{87}Rb/^{86}Sr$ | $\pm 2\sigma$ | $^{87}Sr/^{86}Sr$ | $\pm 2\sigma$ | $^{87}Sr/^{86}Sr_i$ |
|---|---|---|---|---|---|---|---|
| *Sample SG5.413.1 Biotite schist. 54.7820 S, 35.8095 W.* | | | | | | | |
| *Bt–titanite isochron 83.7 ± 1.2 Ma* | | | | | | | |
| Biotite | 274.95 | 13.72 | 58.39 | 0.8758 | 0.778251 | 0.000022 | 0.709394 |
| Titanite | 2.20 | 44.23 | 0.14 | 0.0022 | 0.708968 | 0.000061 | 0.708798 |

Age calculated using the $^{87}Rb$ decay constant of $1.42 \times 10^{-11}$ (Steiger and Jäger, 1977).

$^{87}Sr/^{86}Sr$ $2\sigma$ analytical uncertainties in Table 1 were used for the age calculations. During analysis the SRM 987 Sr standard yielded a $^{87}Sr/^{86}Sr$ ratio of 0.710241 ± 18 ($2\sigma$, $n = 6$).

Biotite forms the $S_1$ foliation together with MS1 to MP1 titanite yield a Rb-Sr isochron of 83.7 ± 1.2 Ma. Although some of the titanite analysed may have formed after biotite, the open nature of Rb and Sr in biotite mean it was likely in isotopic equilibrium with the biotite. Moreover, the moderately high Rb/Sr mean there is less dependence on titanite as an initial ratio, meaning that in all likelihood the age is reliable and records isotopic closure after the first deformation event.

### 4.2. U-Pb zircon geochronology

U-Pb zircon geochronology on granite samples SG5.188.1 and SG5.294.1 (Table 2) was carried out at the NORDSIM facility using the Cameca 1270 ion-microprobe housed at the Swedish Museum of Natural History. The zircons separated were bright prisms generally about 200 μm long with aspect ratios of 2:1 and well-formed crystal facets. After mounting the zircons into epoxy and polishing to expose the interiors of the grains, the mount was introduced into an SEM. Under cathodo-luminescence (CL) the grains exhibited fine growth zoning that is a typical texture for zircon growing from granitic magma (Corfu et al., 2003). Rare zircon inheritance was identified from the CL images as distinct cores, often less luminescent than the rim overgrowths. The greater majority of the grains were simple and with no inheritance. The CL images were then used to choose analysis spots once the mount was introduced into the ion-microprobe. The automated procedure outlined by Whitehouse and Kamber (2005) was followed for these analyses: a defocused primary $O_2$-ion beam resulted in elliptical analysis spots 20 μm in diameter. Measured Pb/U ratios, elemental concentrations and Th/U ratios were calibrated relative to the Geostandards zircon 91500, which has an age of 1065 Ma (Wiedenbeck et al., 1995). Ages were calculated using isoplot (Ludwig, 2003).

Nine of the ten analyses from sample SG5.188.1 yield a concordia age of 160.2 ± 0.9 Ma (Fig. 11). The remaining analysis comes from an inherited core which yields a $^{206}Pb/^{238}U$ age of 186.1 ± 3.1 Ma. Eight of ten analyses from sample SG5.294.1 yield a concordia age of 160.0 ± 1.4 Ma (Fig. 11). The other analyses were excluded because they either represented an older inherited grain or contained common Pb and had suffered recent Pb loss. As the precision of the SIMS zircon geochronology method is likely to be no less than 1% (e.g. Stern and Amelin, 2003) we consider the ages of the two granites to be indistinguishable at 160 ± 2 Ma.

## 5. The structural and kinematic evolution of the Cooper Bay Formation and the timing of its development

The sinistral, strike-slip Cape Vahsel Shear Zone has played a critical role in partitioning deformation within the Cooper Bay Formation, with $D_1$ strain increasing significantly from northeast

**Table 2**
U-Pb ion-microprobe zircon data.

| Spot[a] | U (ppm) | Th (ppm) | Pb (ppm) | Th/U | $f^{206}$ (%)[b] | $^{238}U/^{206}Pb$ | ±σ (%) | $^{207}Pb/^{206}Pb$ | ±σ (%) | $^{206}Pb/^{238}U$ age (Ma) | ±σ | $^{207}Pb/^{206}Pb$ age (Ma)[c] | ±σ |
|---|---|---|---|---|---|---|---|---|---|---|---|---|---|
| *SG.188.1. Granite. LAT, LONG. Concordia age 160.0 ± 1.4 Ma* | | | | | | | | | | | | | |
| 1* | 275 | 106 | 8 | 0.385 | 0.11 | 40.002 | 0.83 | 0.04907 | 2.57 | 159.2 | 1.3 | 159.2 | 1.3 |
| 2* | 318 | 138 | 9 | 0.435 | 0.24 | 39.919 | 0.79 | 0.05006 | 2.50 | 159.1 | 1.2 | 159.3 | 1.3 |
| 3* | 1122 | 836 | 37 | 0.745 | 0.07 | 38.930 | 1.15 | 0.04945 | 1.26 | 163.4 | 1.9 | 163.5 | 1.9 |
| 4* | 543 | 244 | 16 | 0.450 | 0.15 | 39.635 | 0.85 | 0.05023 | 1.77 | 160.4 | 1.3 | 160.4 | 1.4 |
| 5* | 1513 | 559 | 44 | 0.370 | 0.11 | 39.431 | 0.92 | 0.04942 | 1.08 | 161.3 | 1.5 | 161.4 | 1.5 |
| 6* | 269 | 165 | 8 | 0.615 | 0.23 | 40.018 | 0.98 | 0.05029 | 2.53 | 158.8 | 1.5 | 158.9 | 1.6 |
| 7i | 243 | 90 | 8 | 0.369 | 0.14 | 34.138 | 0.84 | 0.04821 | 2.47 | 186.1 | 1.5 | 186.5 | 1.6 |
| 8* | 362 | 220 | 11 | 0.607 | 0.20 | 40.365 | 0.83 | 0.04818 | 2.22 | 157.4 | 1.3 | 158.0 | 1.3 |
| 9* | 309 | 107 | 9 | 0.347 | 0.30 | 39.349 | 0.82 | 0.04918 | 2.35 | 161.3 | 1.3 | 161.8 | 1.3 |
| 10* | 293 | 113 | 9 | 0.384 | 0.31 | 39.838 | 0.81 | 0.05001 | 2.47 | 159.3 | 1.3 | 159.7 | 1.3 |
| *SG.294.1. Granite. LAT, LONG. Concordia age 160.2 ± 0.9 Ma* | | | | | | | | | | | | | |
| 1* | 335 | 197 | 10 | 0.589 | 0.29 | 39.999 | 0.83 | 0.04806 | 2.33 | 158.7 | 1.3 | 159.4 | 1.3 |
| 2* | 827 | 458 | 26 | 0.553 | 0.59 | 39.285 | 1.03 | 0.05292 | 2.42 | 161.1 | 1.6 | 161.3 | 1.7 |
| 3* | 413 | 185 | 12 | 0.448 | 0.27 | 39.921 | 0.97 | 0.04978 | 2.05 | 159.1 | 1.5 | 159.4 | 1.6 |
| 4 | 372 | 145 | 10 | 0.389 | 25.31 | 30.944 | 1.65 | 0.24368 | 7.72 | 153.8 | 4.2 | 154.6 | 8.6 |
| 5* | 1023 | 694 | 33 | 0.678 | 0.09 | 39.029 | 0.88 | 0.04987 | 1.30 | 162.9 | 1.4 | 163.0 | 1.4 |
| 6* | 712 | 293 | 21 | 0.411 | 0.08 | 39.960 | 0.79 | 0.04847 | 1.59 | 159.2 | 1.2 | 159.5 | 1.3 |
| 7* | 491 | 197 | 14 | 0.401 | 0.21 | 40.115 | 0.83 | 0.04836 | 1.90 | 158.4 | 1.3 | 158.9 | 1.3 |
| 8* | 156 | 46 | 4 | 0.298 | 0.71 | 40.472 | 0.79 | 0.05048 | 3.94 | 156.2 | 1.2 | 157.1 | 1.3 |
| 9i | 696 | 262 | 56 | 0.376 | 0.03 | 14.484 | 0.84 | 0.05623 | 0.92 | 430.2 | 3.5 | 429.9 | 3.5 |
| 10* | 901 | 442 | 28 | 0.491 | 0.10 | 39.374 | 0.79 | 0.04937 | 1.64 | 161.5 | 1.3 | 161.7 | 1.3 |

Calculations were made using Isoplot 3.1 (Ludwig, 2003) and used the decay constants of Steiger and Jäger (1977).
[a] Analysis identification. Asterisks are included in age calculations, i indicates inherited grains.
[b] Percentage of common $^{206}Pb$ estimated from the measured $^{204}Pb$. Data is not corrected for common Pb.
[c] Derived by correcting for common Pb assuming a $^{207}Pb/^{206}Pb$ value of 0.83 (present day terrestrial average of Stacey and Kramers (1975)).

to southwest across it, while $D_2$ structures are largely confined to its southwest.

In the Cape Vahsel area, the general clockwise obliquity of $F_1$ folds, combined with the counter-clockwise rotation and enhancement of $D_1$ fabrics adjacent to the CVSZ, suggests that $D_1$ deformation in the Cape Vahsel area was wrench dominated and synchronous with sinistral shear along the CVSZ (Fig. 12).

To the southwest of the CVSZ, $D_1$ structures are higher strain and have been significantly modified by $D_2$ folding. However, $D_1$

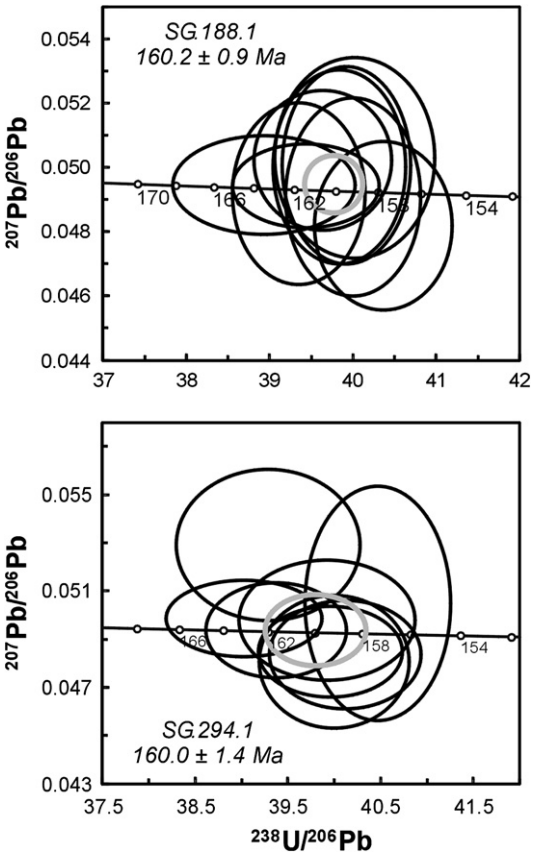


**Fig. 11.** Concordia diagrams of U-Pb geochronology. Analyses of inherited grains and those with common Pb and/or recent Pb loss are omitted.

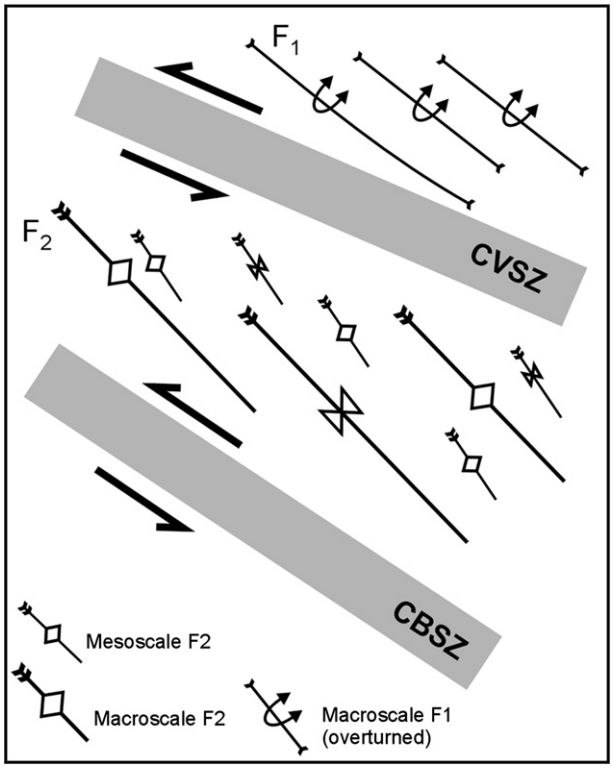


**Fig. 12.** Schematic diagram summarising the mean relationship of principal structures within the Cape Vahsel and Cooper Bay area relative to the regional shear zones. CVSZ – Cape Vahsel Shear Zone, CBSZ – Cooper Bay shear zone. Fold generation denoted by number of 'ticks' on fold trace.

structures do share some important similarities to the most highly strained structures at Cape Vahsel, with the mean $L_1$ mineral lineation and $F_1$ fold hinges being sub-parallel (Fig. 10). Unfortunately, due to the effects of $D_2$ deformation it is unclear if this relationship is attributable to a component of homogeneous sinistral deformation. However, rare examples of $S_1$-parallel, shear band arrays were encountered that betray the presence of non-coaxial shear along the composite $S_1$ foliation plane, and sub-parallel to the $L_1$ mineral lineation. In examples where $S_1$ was steeply inclined the shear band array exhibits a sinistral sense of shear, whereas in areas of shallowly inclined $S_1$, a top to the southeast, strike-parallel sense of shear is observed. If the original attitude of these $F_1$ folds is assumed to be upright, as at Cape Vahsel, restoration of the composite $S_1$ fabric to sub-vertical reveals that all shear band arrays encountered would have exhibited a sinistral sense of shear prior to $F_2$ refolding, providing evidence for a distributed, and possibly significant, component of sinistral shear during $D_1$ deformation of the Cooper Bay Fm.

$D_1$ structures between the Cooper Bay and Cape Vahsel shear zones became progressively rotated as a prelude to $F_2$ refolding which generated a left-stepping, en echelon array of open to close, macroscale folds that exhibit a mean 12° clockwise-oblique trend to the CBSZ (Figs. 3 and 12). Widespread mesoscale $F_2$ folds form, on average, a larger clockwise-oblique angle to the CBSZ. However, the angle of obliquity between fold axial plane and the CBSZ reduces systematically, in a counter-clockwise sense, with increasing fold tightness, an observation consistent with fold initiation and development in response to a component of distributed sinistral strike-slip deformation parallel to the CBSZ.

The consistent presence of a sinistral wrench component to the deformation of the Cooper Bay Formation and adjacent shear zones indicates that main Andean deformation of the Early Cretaceous back-arc basin of South Georgia was not simply a product of orthogonal closure as previously inferred (Tanner et al., 1981; Macdonald et al., 1987). While our own field data confirm observations from previous field studies (Dalziel et al., 1975; Stone, 1980) that the intensely folded Cumberland Bay and Sandebugten formations display an approximately orthogonal mean mineral stretching lineation (trend 025°) relative to the regional fold axis and cleavage trend of N120°E (Fig. 2), the existence of contemporaneous strike-parallel sinistral shear along the CBSZ is indicative of kinematically partitioned transpressional deformation (Dewey et al., 1998 and references therein).

Kinematic partitioning can be manifest to various degrees and styles from simple partitioning of the coaxial and non-coaxial components, to continuous partitioning (asymmetric or symmetric), or discontinuous partitioning (Dewey et al., 1998). Although the degree of partitioning within a transpressional orogen has been modelled with some success (Teyssier et al., 1995), we lack the constraints on plate motion and instantaneous strain axes to estimate the efficiency of the kinematic strain partitioning in South Georgia. However, it may be possible to characterise the potential strain paths responsible for the wrench-related folding within the Cooper Bay study area allowing the style and pattern of partitioning to be established.

### 5.1. Characterising strain paths and kinematic strain partitioning from fold appression

Field and theoretical studies of en echelon folds have revealed that the orientation of the fold axial plane relative to the shear plane, its rate of subsequent rotation and fold tightening or appression is largely controlled by the strain path followed (Sanderson and Marchini, 1984; Little, 1992). Little (1992) calculated theoretical curves describing the variation of axial plane strike with interlimb angle for simple shear, and specific cases of simple transpression and incremental transtension (Fig. 13a), using the model assumptions of Sanderson and Marchini (1984). Although, based on a simplistic strain model, careful data selection from the four structural domains in the Cooper Bay–Cape Vahsel area enables us to characterise the possible strain paths experienced by the various fold phases (assuming constant relative displacement direction during deformation) and thus estimate how the coaxial and non-coaxial components of transpressional strain are partitioned.

The fold orientation and interlimb angle data presented in Fig. 13 represent folds of meso- (decimetre to metre scale) to macroscale (decametre to hundreds of metre scale), formed during two phases of deformation. Mesoscale folds were systematically recorded by measurement of axial plane, fold hinge and symmetry, while tightness was recorded according to standard fold tightness classification scheme and not as a specific value. As a consequence we are unable to plot axial plane strike against actual interlimb angle for individual folds. Instead the mean axial plane was calculated for all mesoscale folds within a specific range of fold tightness and this mean axial plane strike is plotted against the median interlimb angle of the specific range of fold tightness (e.g. tight folds range between 1 and 30°, with median of 15°). For macroscale folds the interlimb angle for individual folds was calculated from cross section and, as they predominantly fell within a single defined range of fold tightness, was averaged. The azimuth of the mean fold axis, determined from stereographic data analysis, is used as a proxy for mean axial plane strike as the folds are overwhelmingly upright in attitude.

#### 5.1.1. Macroscale folds in the Cooper Bay Fm

The macroscale $F_1$ folds developed in the Cooper Bay Fm. at Cape Vahsel possess interlimb angles that are almost exclusively $<33°$, and have a mean of 28°, while the calculated mean fold axis forms a 14° clockwise-oblique angle to the adjacent CVSZ. These mean values plot close to the theoretical strain path for simple shear, although at the relatively high implied strain ($\gamma > 2$) there is considerable overlap with other potential strain paths particularly within the transtensional field (Fig. 13b). Unfortunately, due to the limited range of fold tightness data for these macroscale $F_1$ folds, a robust estimate for the likely strain path is not possible. However assuming a constant relative displacement direction, the fold data is at least consistent with a simple shear deformation path.

The en echelon array of macroscale $F_2$ folds developed between the Cape Vahsel and Cooper Bay shear zones exhibits generally open interlimb angles ranging from 123 to 60° (mean 100°), forming a mean 12° clockwise-obliquity to the CBSZ. These mean values plot well to the right of the simple shear path in Fig. 13b, within the transpressional strain path field. Again the range of fold data is limited, but assuming a constant relative displacement direction, we interpret the fold array as a result of distributed transpressive deformation.

#### 5.1.2. Mesoscale folding in the Cooper Bay Fm

Mesoscale $F_2$ folds are more numerous and exhibit a broad range of interlimb angles enabling us to plot the mean axial plane orientation for five subdivisions of fold interlimb angle to establish a possible deformation path. The mesoscale $F_2$ fold data plot predominantly within error of the simple shear field, with the exception of tight folds that show an excursion toward the transtension field. This excursion may potentially be an artefact of the routine data recording methods employed whereby fold tightness was recorded by descriptive terms rather than exact values. If, as is likely, the actual interlimb angle values for recorded tight folds do not form an even distribution from 30-1°, but rather clustered toward the upper limit, then the actual mean interlimb angle for

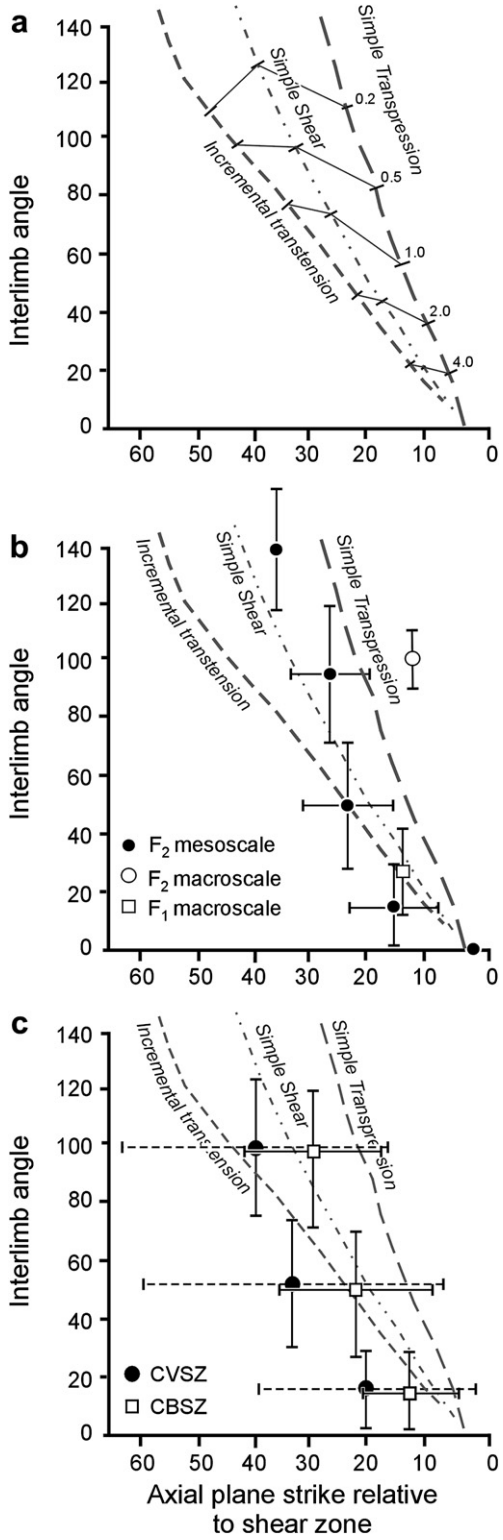


**Fig. 13.** a) Theoretical curves for tightening (appression) and rotation of folds in a simple shear, and specific simple transpression and incremental transtension (redrawn from Little, 1992). 'Contours' along curves denote shear strains along the strain paths. b) Interlimb angle vs axial planar strike angle relative to adjacent shear zone for folds within the Cooper Bay Formation. Open square – macroscale F1 folds in the Cape Vahsel area, open circle – macroscale F2 folds in Cooper Bay area, and filled circle – mesoscale F2 folds in Cooper Bay area. c) plot as above but for mesoscale folds in Cooper Bay Shear Zone - open squares, and Cape Vahsel Shear Zone – filled circles.

the tight folds is likely to be greater than the median value for the classification field. Therefore it is probable that the actual data for tight folds would plot closer to the simple shear strain field.

### 5.1.3. Shear zone folds

Fold data from the Cooper Bay and Cape Vahsel shear zones show a similar distribution to the mesoscale $F_2$ fold population, with folding of the main mylonite fabric in the Cooper Bay shear zone plotting within error along an approximately simple shear strain path, although again data from tight folds shows an excursion toward the transtensional field (Fig. 13c). In comparison, folds developed within the Cape Vahsel Shear Zone plot predominantly within the field of transtensional strain paths, although there is a large degree of error associated with this dataset. While the CVSZ fold data is superficially indicative of a transtensional strain path, this result may be explained by the ubiquitous presence of decimetre-scale C′-type shear bands throughout the CVSZ which are responsible for a component of clockwise rotation, antithetic to the sinistral wrench-related rotation of the fold hinges. This counter rotation effectively reduces the amount of fold rotation toward the shear zone trend relative to fold tightening, potentially explaining the apparent shift to the left when the data are plotted.

### 5.1.4. Interpretation of strain paths

Our analysis of fold appression in the Cooper Bay region reveals a predominance of strain paths approximating simple shear suggesting that the wrench component of Andean age sinistral transpressional deformation was for the most part efficiently partitioned along the regional-scale shear zones, and within adjacent $F_1$ folding of the Cooper Bay Fm. Such efficient kinematic strain partitioning could be the product of wrench-dominated transpression where the angle of relative plate motion is $<20°$ (Teyssier et al., 1995) or due to the presence of a pre-existing large-scale crustal structural architecture (Jones and Tanner, 1995; Holdsworth et al., 2002) such as that inferred prior to the formation of the CBSZ (Tanner et al., 1981).

The en echelon, macroscale $F_2$ fold array that is confined between the Cooper Bay and Cape Vahsel shear zones appears to have been the product of a transpressional strain path. Such temporal and spatial variation in kinematic partitioning within the Cooper Bay area is possibly due to the reorientation of $D_1$ structural anisotropy (composite $S_1$ foliation) from sub-vertical to sub-horizontal prior to development of $F_2$ folding, exemplifying the influence of pre-existing anisotropy and its subsequent structural modification on kinematic partitioning (Tavarnelli et al., 2004).

## 5.2. Timing of shearing

The closure of the Rb-Sr system in biotite, commonly proportioned to cooling below metamorphic temperatures of approximately 300 °C (e.g. Cliff, 1985), is in reality also dependent on many other factors such as composition, availability of suitable sinks, the presence of a fluid and the fluid composition (Villa, 1997). Nevertheless, the general open behaviour for the Rb-Sr system in biotite means that irrespective of the actual cause of isotopic closure in this case, the biotite mineral age will likely record a time shortly after shearing and metamorphism, possibly related to uplift and exhumation of the metamorphic rocks. The $83.7 \pm 1.2$ Ma Rb-Sr biotite–titanite isochron is, therefore, interpreted to record a minimum age for sinistral shearing in the Cooper Bay region. The U-Pb ages for the two granite samples are interpreted to date intrusion of the granites at 160 Ma. As the granites are affected by all the deformation within the Cooper Bay shear zone, they, in combination with the biotite geochronology, limit shearing and the development of the Cooper Bay shear zone between c. 160 and 83 Ma.

## 6. Regional correlations

The geological and tectonic correlations between the island of South Georgia and the Rocas Verdes Marginal Basin (RVMB) in the Fuegian Andes, Patagonia, are well established (e.g. Dalziel et al., 1975; Tanner, 1982; Thomson et al., 1982; Mukasa and Dalziel, 1996), although our new data provide improved geochronological and tectonic correlations.

The c. 160 Ma granodiorite at Cooper Bay forms part of a volumetrically minor suite of granitic rocks intruding and associated with widespread tholeiitic gabbroic plutons of the Drygalski Fjord Complex (Storey, 1983). The granitic rocks form two chemically distinct groups (Storey and Mair, 1982): Oceanic plagiogranites that follow the differentiation trend of the basic rocks, and those that have a transitional chemistry between the plagiogranite and continental calc-alkaline rocks (Storey and Mair, 1982). Storey (1983) noted the compositional similarity between the Cooper Bay granodiorite and calc-alkaline Trendall Crag granodiorite which shares Ce/Y and Ti/Zr ratios similar to that of the Tobífera Formation in Patagonia (Storey and Mair, 1982), U/Pb zircon ages for which suggest it erupted between $178.4 \pm 1.4$ Ma and $171.8 \pm 1.2$ Ma (Pankhurst et al., 2000), until 142 Ma (Calderón et al., 2007) in the northern Rocas Verdes basin. However, our U/Pb zircon age is more closely correlated to the $164 \pm 1.7$ Ma (Mukasa and Dalziel, 1996) peraluminous Darwin granite suite, in the Cordillera Darwin, that has long been considered coeval and possibly cogenetic with the Tobífera Formation (Nelson, 1981). Emplacement of the c. 160 Ma granites occurred during extensive attenuation of the continental margin prior to the formation of the Rocas Verdes back-arc basin (e.g. Storey and Mair, 1982; Calderón et al., 2007) and coincided with the latter V3 stage of silicic large igneous province volcanism associated with the initiation of Gondwana break-up (Pankhurst et al., 2000).

Our new interpretation of the mid to Late Cretaceous age structural development of South Georgia, particularly the Cooper Bay–Cape Vahsel area, considerably strengthens the structural correlation with the mid-Cretaceous main Andean Orogeny (Nelson, 1982; Suarez et al., 2000) which resulted from the closure and inversion of the RVMB. Although some of the sinistral strike-slip structures in the Fuegian Andes are of Cenozoic origin (Cunningham, 1993; Chiglione and Ramos, 2005; Chiglione and Cristallini, 2007; Olivero and Martinioni, 2001; Klepeis and Austin, 1997), in the Cordillera Darwin, Patagonia, as in South Georgia, main Andean deformation is characterised by sinistral transpressional deformation with the wrench component being partitioned along the Beagle Channel (Cunningham, 1995).

In the Cordillera Darwin, a compilation of K–Ar mineral and Rb-Sr whole rock ages, combined with biostratigraphical data constrains the main Andean orogeny to have occurred between 100 and 85 Ma (Hervé et al., 1981). Subsequent U-Pb dating of the 69 Ma Beagle granite which post-dates main Andean deformation fabrics (Mukasa and Dalziel, 1996) supports this interpretation. Our Rb-Sr biotite geochronology is entirely consistent with the Patagonian data, constraining the main Andean deformation event in South Georgia, the D1 deformation at Cooper Bay, as being pre-84 Ma.

Broadly coeval, sinistral transpressional deformation is also present on Elephant Island, South Shetland Islands, at the tip of the Antarctic Peninsula (Trouw et al., 2000). Mid-Cretaceous plate reconstructions for the Scotia Arc place Elephant Island in a complex region between South America and the Antarctic Peninsula (e.g. Grunow et al., 1991; Lawver et al., 1992) in the southern Andean forearc, and in relatively close proximity to the Early Cretaceous marginal basin represented by the RVMB and South Georgia (Fig. 14). It is possible that deformation of Elephant Island may have been associated with sinistral oblique closure of the RVMB (Grunow et al., 1992) and South Georgia, induced by the relative plate motion of South America and Antarctic Peninsula during early evolution of the Scotia Sea, generating a significant component of sinistral strike-slip displacement during the mid-Late Cretaceous (Grunow et al., 1991, 1992; Lawver et al., 1992; Cunningham et al., 1995).

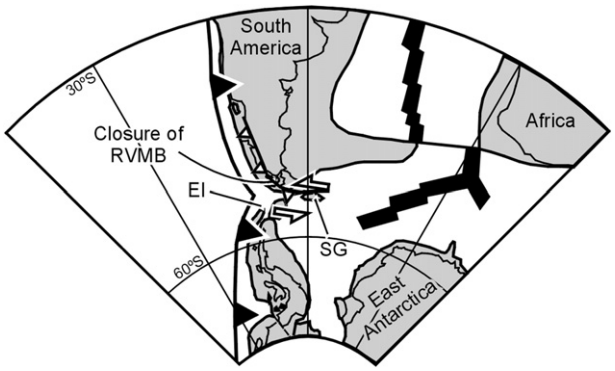


**Fig. 14.** 100 Ma plate reconstruction redrawn from Grunow et al. (1992) with the inclusion of South Georgia (SG). EI – Elephant Island, RVMB – Rocas Verdas Marginal Basin.

## 7. Conclusions

The Cooper Bay area of South Georgia preserves a polyphase deformation history that is intimately associated with orogen-parallel sinistral shear along the Cooper Bay shear zone, which we interpret as the partitioned wrench component of bulk transpressional deformation during the mid-Cretaceous main Andean orogeny.

The Cooper Bay shear zone exhibits a complex kinematic history with both normal and reverse dip-slip shear preserved within plutonic basement lithologies, with a broad zone of sinistral strike-slip shear developed within metagreywackes of the Cooper Bay Formation. Regional scale deformation of the Cooper Bay Formation is compartmentalised by the newly identified sinistral Cape Vahsel Shear Zone, with higher D1 and D2 strains developed between the two shear zones than found to the northeast of the CVSZ. The relationship between fold axial plane orientation and interlimb angle for various spatial and temporally related folds is consistent with counter-clockwise rotation and fold appression as a result of a sinistral simple shear deformation path, suggesting kinematic strain partitioning of the wrench component was highly efficient. Locally, the modification of steep tectonic anisotropies to shallow inclinations during D2 deformation induced imperfect or inefficient partitioning with fold arrays exhibiting fold appression characteristic of a transpressional deformation path.

New U-Pb zircon and Rb-Sr biotite dates constrain shearing and the development of the Cooper Bay shear zone between 160 and 83 Ma. The 83 Ma Rb-Sr biotite date is interpreted as recording uplift and exhumation shortly after D1 shearing and metamorphism of the Cooper Bay Formation.

Our new geochronological age constraints and partitioned transpression model for main Andean deformation of South Georgia provides enhanced mid-Cretaceous tectonic correlations with the Cordillera Darwin, Patagonia.

## Acknowledgements

The Captain and crew of HMS Endurance are thanked for logistical support during the field campaign, while Kirk Watson

provided excellent field assistance. Rudolf Trouw and Bryan Storey are thanked for constructive reviews. This study was funded by the Natural Environment Research Council and is part of the British Antarctic Survey's Polar Science for Planet Earth Programme. This is Nordsim publication number 250, the Nordsim facility is operated under an agreement between the Swedish Museum of Natural History, the Geological Survey of Finland and the research funding agencies of Denmark, Sweden and Norway.

## References

Berthé, D., Choukroune, P., Gapais, D., 1979. Orientations préférentialles du quartz et orthogeniessification progressive en régime cisaillant. Bulletin of Mineralogy 102, 265–272.

Bruhn, R.L., Dalziel, I.W.D., 1977. Destruction of the Early Cretaceous marginal basin in the Andes of Tierra del Fuego. In: Talwani, M., Pitman, W.C. (Eds.), Island Arcs, Deep Sea Trenches and Back-Arc Basins. Maurice Ewing Series 1. AGU, Washington D.C., pp. 395–405.

Calderón, M., Fildani, A., Hervé, F., Fanning, C.M., Weislogel, A., Cordani, U., 2007. Late Jurassic bimodal magmatism in the northern Sea-floor remnant of the Rocas Verdes basin, southern Patagonian Andes. Journal of the Geological Society, London 164, 1011–1022.

Chiglione, A.C., Cristallini, E.O., 2007. Have the southernmost Andes been curved since Late Cretaceous time? An analogue test for the Patagonia Orocline. Geology 35, 13–16.

Chiglione, A.C., Ramos, V.A., 2005. Progression of deformation and sedimentation in the southernmost Andes. Tectonophysics 405, 25–46.

Clayton, R.A.S., 1982. A preliminary investigation of the Geochemistry of greywackes from South Georgia. British Antarctic Survey Bulletin 51, 89–109.

Cliff, R.A., 1985. Isotopic dating in metamorphic belts. Journal of the Geological Society, London 142, 97–110.

Corfu, F., Hanchar, J.M., Hoskin, P.W.O., Kinny, P., 2003. Atlas of zircon textures. In: Hanchar, J.M., Hoskin, P.W.O. (Eds.), Zircon. Reviews in Mineralogy and Geochemistry, vol. 53. Mineralogical Society of America, Geochemical Society, pp. 468–500.

Cunningham, W.D., 1993. Strike-slip faults in the southernmost Andes and development of the Patagonian Orocline. Tectonics 12, 169–186.

Cunningham, W.D., 1995. Orogenesis at the southern tip of the Americas: the structural evolution of the Cordillera Darwin metamorphic complex, southernmost Chile. Tectonophysics 244, 197–229.

Cunningham, W.D., Dalziel, I.W.D., Lee, T.-Y., Lawver, L.A., 1995. Southernmost South America–Antarctic Peninsula relative plate motions since 84 Ma: implications for the tectonic evolution of the Scotia Arc region. Journal of Geophysical Research 100, 8257–8266.

Curtis, M.L., 2007. Main Andean sinistral shear along the Cooper Bay Dislocation Zone, South Georgia? In: Cooper, A.K., Raymond, C.R., et al. (Eds.), Antarctica: A Keystone in a Changing World – Online Proceedings of the 10th ISAES. USGS Open-File Report 2007-1047, Short Research Paper 034. doi:10.3133/of2007-1047.srp034, 4 pp.

Dalziel, I.W.D., 1981. Back-arc extension in the southern Andes: a review and critical reappraisal. Philosophical Transactions of the Royal Society of London, Series A 300, 319–335.

Dalziel, I.W.D., 1986. Collision and cordilleran orogenesis: an Andean perspective. In: Coward, M.P., Ries, A.C. (Eds.), Collision Tectonics. Geological Society, London, Special Publication, vol. 19, pp. 389–404.

Dalziel, I.W.D., 1992. Antarctica; a tale of two supercontinents. Annual Review of Earth and Planetary Sciences 20, 501–526.

Dalziel, I.W.D., Dott, R.H., Winn, R.D., Bruhn, R.L., 1975. Tectonic relations of South Georgia Island to the southernmost Andes. Geological Society of America Bulletin 86, 1034–1040.

Dewey, J.F., Holdsworth, R.E., Strachan, R.A., 1998. Transpression and transtension zones. In: Holdsworth, R.E., Strachen, R.A., Dewey, J.F. (Eds.), Continental Transpressional and Transtensional Tectonics. Geological Society, London, Special Publications, vol. 135, pp. 1–14.

Dott, R.H., Winn, R.D., Smith, C.H.L., 1982. Relationship of Late Mesozoic and Early Cenozoic sedimentation to the Tectonic evolution of the southernmost Andes and Scotia Arc. In: Craddock, C. (Ed.), Antarctic Geoscience. University of Wisconsin Press, Madison, pp. 193–202.

Fildani, A., Hessler, A.M., 2005. Stratigraphic record across a retroarc basin inversion: Rocas verdes–Magellanes Basin, Patagonian Andes, Chile. Geological Society of America Bulletin 117, 1596–1614.

Grunow, A.M., Dalziel, I.W.D., Harrison, T.M., Heizler, M.T., 1992. Structural geology and geochronology of subduction complexes along the margin of Gondwanaland: new data from the Antarctic Peninsula and southernmost Andes. Geological Society of America Bulletin 104, 1497–1514.

Grunow, A.M., Kent, D.V., Dalziel, I.W.D., 1991. New paleomagnetic data from Thurston Island: implications for the tectonics of West Antarctica and Weddell Sea opening. Journal of Geophysical Research 96, 17935–17954.

Hervé, F., Nelson, E., Kawashita, K., Suárez, M., 1981. New isotopic ages and the timing of orogenic events in the Cordillera Darwin, southernmost Chilean Andes. Earth and Planetary Science Letters 55, 257–265.

Holdsworth, R.E., Tavarnelli, E., Clegg, P., Pinheiro, R.V.L., Jones, R.R., McCaffrey, K.-J.W., 2002. Domainal deformation patterns and strain partitioning during transpression: an example from the Southern Uplands terrane, Scotland. Journal of the Geological Society, London 159, 401–415.

Jones, R.R., Tanner, P.W.G., 1995. Strain partitioning in transpression zones. Journal of Structural Geology 17, 793–802.

König, M., Jokat, W., 2006. The Mesozoic breakup of the Weddell Sea. Journal of Geophysical Research 111, B12102. doi:10.1029/2005JB004035.

Klepeis, K.A., Austin, J.A., 1997. Contrasting styles of superimposed deformation in the southernmost Andes. Tectonics 16, 755–776.

Lawver, L.A., Gahagan, L.M., Coffin, M.F., 1992. The development of palaeoseaways around Antarctica. In: Kennett, J.P., Warnke, D. (Eds.), The Antarctic Palaeoenvironment: A Perspective on Global Change. Antarctic Research Series, vol. 56. AGU, Washington D.C., pp. 7–30.

Little, T.A., 1992. Development of wrench folds along the Border Ranges fault system, southern Alaska, U.S.A. Journal of Structural Geology 14, 343–359.

Livermore, R., Hillenbrand, C.-D., Meredith, M., Eagles, G., 2007. Drake passage and Cenozoic climate: an open and shut case? Geochemistry, Geophysics, Geosystems 8, Q01005. doi:10.1029/2005GC001224.

Ludwig, K.R., 2003. User Manual for isoplot 3.00: a Geochronological Toolkit for Microsoft Excel. In: Berkeley Geochronology Centre Special Publications, vol. 4 1–70.

Macdonald, D.I.M., Storey, B.C., Thomson, J.W., 1987. South Georgia, BAS GEOMAP Series, Sheet 1, 1:250,000, Geological Map and Supplementary Text. British Antarctic Survey, Cambridge, 63 pp.

Mair, B.F., 1987. The Geology of South Georgia: VI. Larsen Harbour Formation. British Antarctic Survey Scientific Reports No. 111, 60 pp.

Mukasa, S.B., Dalziel, I.W.D., 1996. Southermost Andes and South Georgia Island, North Scotia Ridge: zircon U-Pb and muscovite $^{40}Ar/^{39}Ar$ age constraints on tectonic evolution of Southwestern Gondwanaland. Journal of South American Earth Sciences 9, 349–365.

Nelson, E.P., 1981. Geological evolution of the Cordillera Darwin orogenic core complex, southern Andes. PhD Thesis, New York, Columbia University.

Nelson, E.P., 1982. Post-tectonic uplift of the Cordillera Darwin orogenic core complex: evidence from fission track geochronology and closing temperature–time relationships. Journal of the Geological Society, London 139, 755–761.

Nelson, E.P., Dalziel, I.W.D., Milnes, A.G., 1980. Structural geology of the Cordillera Darwin – collisional-style orogenesis in the southernmost Chilean Andes. Eclogae Geologicae Helvetiae 73, 727–751.

Olivero, E.B., Martinioni, D.R., 2001. A review of the geology of the Argentinian Fuegian Andes. Journal of South American Earth Sciences 14, 175–188.

Pankhurst, R.J., Riley, T.R., Fanning, C.M., Kelley, S.P., 2000. Episodic silicic volcanism in Patagonia and the Antarctic Pensinsula: chronology of magmatism associated with the break-up of Gondwana. Journal of Petrology 41, 605–625.

Sanderson, D.J., Marchini, W.R.D., 1984. Transpression. Journal of Structural Geology 6, 449–458.

Skidmore, M.J., 1972. The geology of South Georgia: III. Prince Olav Harbour and Stromness Bay areas. British Antarctic Survey Scientific Reports 73, 50 pp.

Stacey, J.S., Kramers, J.D., 1975. Approximation of terrestrial lead evolution by a two-stage model. Earth and Planetary Sciences 26, 207–221.

Steiger, R.H., Jäger, E., 1977. Subcommission on geochronology; convention on the use of decay constants in geo- and cosmochronology. Earth and Planetary Science Letters 36, 359–362.

Stern, R.A., Amelin, Y., 2003. Assessment of errors in SIMS zircon U-Pb geochronology using a natural zircon standard and NIST SRM 610 glass. Chemical Geology 197, 111–142.

Stone, P., 1980. The geology of South Georgia: IV. Barff Peninsula and Royal Bay areas. British Antarctic Survey Scientific Reports 96, 45 pp.

Stone, P., 1982. Geological observations in the Cooper Bay–Wirik Bay area, South Georgia. British Antarctic Survey Bulletin 36, 129–131.

Storey, B.C., 1983. The geology of South Georgia: V. Drygalski Fjord Complex. British Antarctic Survey Scientific Reports 107, 88 pp.

Storey, B.C., Mair, B.F., Bell, C.M., 1977. The occurrence of Mesozoic oceanic floor and ancient continental crust on South Georgia. Geological Magazine 114, 203–208.

Storey, B.C., Mair, B.F., 1982. The composite floor of the Cretaceous back-arc basin of South Georgia. Journal of the Geological Society, London 139, 729–737.

Suárez, M., De La Cruz, R., Bell, C.M., 2000. Timing and origin of deformation along the Patagonian fold and thrust belt. Geological Magazine 137, 345–353.

Tanner, P.W.G., Macdonald, D.I.M., 1982. Models for the deposition and simple shear deformation of a turbidite sequence in the South Georgia portion of the southern Andes back-arc basin. Journal of the Geological Society, London 139, 739–754.

Tanner, P.W.G., Rex, D.C., 1979. Timing of events in an Early Cretaceous Island arc-marginal basin system on South Georgia. Geological Magazine 116, 167–179.

Tanner, P.W.G., 1982. Geological evolution of South Georgia. In: Craddock, C. (Ed.), Antarctic Geoscience. University of Wisconsin Press, Madison, pp. 167–176.

Tanner, P.W.G., Storey, B.C., Macdonald, D.I.M., 1981. Geology of an Upper Jurassic–Lower Cretaceous island-arc assemblage in Hauge Reef, the Pickersgill Islands and adjoining areas of South Georgia. British Antarctic Survey Bulletin 53, 77–117.

Tavarnelli, E., Holdsworth, R.E., Clegg, P., Jones, R.R., McCaffrey, K.J.W., 2004. The anatomy and evolution of a transpressional imbricate zone, Southern Uplands, Scotland. Journal of Structural Geology 26, 1341–1360.

Teyssier, C., Tikoff, B., Markley, M., 1995. Oblique plate motion and continental tectonics. Geology 23, 447–450.

Thomson, M.R.A., Tanner, P.W.G., Rex, D.C., 1982. Fossil and radiometric evidence for ages of deposition and metamorphism of the sedimentary sequences on South Georgia. In: Craddock, C. (Ed.), Antarctic Geoscience. University of Wisconsin Press, Madison, pp. 177–184.

Trouw, R.A.J., Passchier, C.W., Valeriano, C.M., Simões, L.S.A., Paciullo, F.V.P., Ribeiro, A., 2000. Deformational evolution of a Cretaceous subduction complex: Elephant Island, South Shetland Islands, Antarctica. Tectonophysics 319, 93–110.

Villa, I.M., 1997. Isotopic Closure. Terra Nova 10, 42–47.

White, S.H., Burrows, S.E., Carreras, J., Shaw, N.D., Humphreys, F.J., 1980. On mylonites in ductile shear zones. Journal of Structural Geology 2, 175–187.

Whitehouse, M.J., Kamber, B.S., 2005. Assigning dates to thin gneissic veins in high-grade metamorphic terranes: a cautionary tale from Akilia, southwest Greenland. Journal of Petrology 46, 291–318.

Wiedenbeck, M., Alle, P., Corfu, F., Griffin, W.L., Meirer, M., Oberli, F., Von Quadt, A., Roddick, J.C., Spiegel, W., 1995. Three natural zircon standards for U–Th–Pb, Lu–Hf, trace element and REE analyses. Geostandards Newsletter 19, 1–23.